

DOI:10.1002/ejic.201500148

Modulating Sonogashira Cross-Coupling Reactivity in Four-Coordinate Nickel Complexes by Using Geometric Control

Anette Petuker,^[a] Christian Merten,^{*[b]} and Ulf-Peter Apfel^{*[a]}

Keywords: Cross-coupling / Nickel / Tripodal ligands / Silicon / Alkynes

Herein, we present the synthesis of nickel complexes with tripodal phosphine ligands, $\text{CH}_3\text{Si}(\text{CH}_2\text{PPh}_2)_3$ and $\text{CH}_3\text{C}(\text{CH}_2\text{PPh}_2)_3$, and their application as catalysts in Sonogashira cross-coupling reactions in water. Although both types of nickel complexes are based on similar tripodal ligands, the Si-derived compounds adopt stable tetrahedral coordination geometries, whereas the C-derived counterparts adopt a square-planar coordination environment. This structural and electronic difference has an important effect on the catalytic

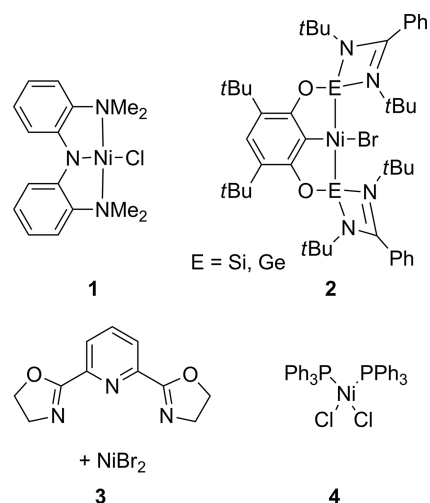
properties of the complexes. Our study demonstrates that C-derived complexes are catalytically inactive, whereas the complexes $[\text{CH}_3\text{Si}(\text{CH}_2\text{PPh}_2)_3\text{NiX}_2]$ ($\text{X} = \text{Cl}^-, \text{Br}^-$) are competent catalysts for cross-coupling reactions of aryl halides with phenylacetylenes. This investigation reveals the importance of structural tuning on catalysis and strongly supports the theory that tetrahedral $(\text{PR}_3)_2\text{NiCl}_2$ complexes are the active species in Sonogashira cross-coupling reactions.

Introduction

Sonogashira cross-coupling reactions are a convenient method to incorporate alkynes into arenes, which are structures commonly found in biologically active molecules, conjugated polymers, and organic photosensitizers.^[1–3] Palladium complexes, such as $\text{Pd}(\text{PPh}_3)_4$, $\text{Pd}(\text{PPh}_3)_2\text{Cl}_2$, $\text{Pd}(\text{dppe})\text{Cl}_2$, and $\text{Pd}(\text{dppp})\text{Cl}_2$, are frequently used for C–C-bond-formation chemistry and are compatible with a wide variety of alkynes as well as aryl iodides, bromides, and triflates.^[4–7] Recently, the groups of Fu,^[8] Glorius,^[9] and Hu^[10,11] extended the substrate scope of Pd-catalyzed coupling reactions to work with non-activated alkyl halides by utilizing N-heterocyclic carbene ligands. However, because of the high cost and possible toxicity of palladium in industrial synthesis, the use of nickel as a cheap, widely available, and less toxic metal is more desirable.^[12,13]

In contrast to palladium catalysis, examples of nickel-catalyzed Sonogashira reactions are still rare, and their mechanisms are poorly understood. General structural and electronic requirements for Ni-based catalysts are unknown. In the few studies available, Hu et al. described the coupling of non-activated alkyl halides, utilizing the Ni^{II}

pincer complex **1** (Scheme 1).^[10] The participation of a Ni^{IV} species in the catalytic cycle was suggested,^[14] and structural as well as spectroscopic evidence for a transmetalation process of a Ni^{II} species as the first step within this coupling process was provided.^[11] These results were further supported by recent findings of the groups of Hartwig and Driess, who used the [ECE] pincer complexes **2** (Scheme 1).^[14] Liu et al. described the nickel-catalyzed Sonogashira coupling of non-activated secondary alkyl bromides and iodides with bis(oxazoline) **3** in the presence of nickel bromide.^[15]



Scheme 1. Literature-known nickel catalysts for the Sonogashira coupling.^[10,11,14,16]

[a] Anorganische Chemie I, Ruhr Universität Bochum, Universitätsstraße 150, 44801 Bochum, Germany
E-mail: ulf.apfel@rub.de
<http://www.ruhr-uni-bochum.de/smallmolecules>

[b] Organische Chemie II, Ruhr Universität Bochum, Universitätsstraße 150, 44801 Bochum, Germany
E-mail: christian.merten@rub.de
<http://www.ruhr-unibochum.de/chirality>

Supporting information for this article is available on the WWW under <http://dx.doi.org/10.1002/ejic.201500148>.

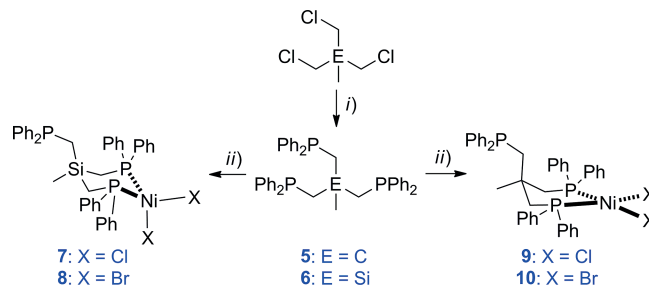
Although $(PR_3)_2PdCl_2$ complexes are effective catalysts for Sonogashira couplings,^[5–7] and although $(PR_3)_2Ni^{II}X_2$ complexes ($X = Cl^-$, Br^- ; $R =$ alkyl, aryl) are commonly used pre-catalysts,^[17–21] only $Ni(PPh_3)_2Cl_2$ (**4**) allowed for an efficient synthesis of tolanes through Sonogashira coupling.^[16,22] Unlike in the case of palladium, nickel complexes of bidentate ligands as well as electron-rich monodentate ligands did not afford the respective tolanes. This exemplifies the limitations of the investigated nickel phosphine complexes for this process.^[16] It was suggested that the strong coordination of nickel to alkynes is a key problem associated with Ni-based Sonogashira catalysis.^[23]

Because $(PPh_3)_2NiCl_2$ can exist in either square-planar or tetrahedral geometry,^[24,25] it is unclear whether or not both conformational isomers are catalytically active. In a report on the stereoselective heterodimerization of styrene and propene catalyzed by tripodal Ni^{II} complexes,^[26] it was shown that tetrahedral Ni complexes were able to perform catalytic heterodimerization reactions, whereas the square-planar analogues could not. Inspired by these results, we became interested in using tripodal phosphine ligands in Sonogashira reactions. We take advantage of the fact that tripodal phosphine ligands can enforce either square-planar or tetrahedral geometry, which depends on the identity of the central atom (i.e., carbon or silicon). To the best of our knowledge, this work presents the first evidence that tetrahedral $(PR_3)_2Ni^{II}X_2$ moieties are an essential prerequisite for successful Ni–phosphine-based Sonogashira cross-coupling reactions.

Results and Discussion

By following established synthesis routes, diphenylphosphine was deprotonated and allowed to react with 1,3-dichloro-2-(chloromethyl)-2-methylpropane to afford the tripodal phosphine Triphos (compound **5**).^[27] Likewise, tris(chloromethyl)methylsilane^[28] reacts with $LiPPh_2$ to afford $Triphos^{Si}$ (compound **6**).

The reaction of **6** with $NiCl_2$ or $(PPh_3)_2NiCl_2$ ^[29] gives the complex $[(Triphos^{Si})NiCl_2]$ (**7**) in approximately 75% yield as a dark red, crystalline solid. Similarly, when **6** is treated with $NiBr_2$, the complex $[(Triphos^{Si})NiBr_2]$ (**8**) can be obtained in 55% yield (Scheme 2). The molecular structures of **7** (Figure 1) and **8** (Figure S1) comprise tetrahedral Ni^{II} centers bearing two phosphine and two chlorido ligands. Ligand **6** coordinates in a bidentate mode, which leaves one free diphenylphosphine group. The Coordination of $CH_3Si(CH_2PPh_2)_2$ to Ni leads to a six-membered ring chelate that adopts a chair conformation. This coordination mode is surprising, as it differs from a square-planar $(PR_3)_2Ni^{II}X_2$ species obtained with the carbon-derivative **9** as a ligand, as reported by McGrady et al.^[30] Contrary to complexes **7** and **8**, the reaction of NiX_2 with ligand **5** afforded the square-planar complexes $[(Triphos)NiCl_2]$ (**9**) and $[(Triphos)NiBr_2]$ (**10**) in the solid state (Scheme 2).



Scheme 2. Synthesis of tripodal phosphines and their Ni complexes. (i) *n*BuLi, THF, HPPPh₂, –78 °C; (ii) NiX₂ (X = Cl[–], Br[–]), DMF/THF (1:1).

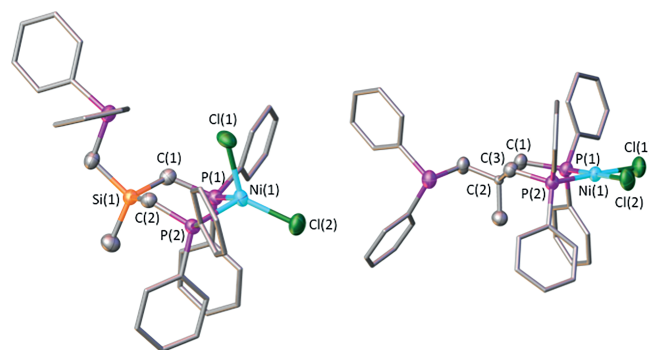


Figure 1. Molecular structures of compounds **7** (left) and **9** (right) with thermal ellipsoids drawn at the 50% probability level (hydrogen atoms and thermal ellipsoids of the phenyl groups are omitted for clarity).

A detailed bonding analysis of **7** and **9** shows that the Ni–P distances significantly decrease [from ca. 2.296 (for **7**) to 2.179 Å (for **9**)] upon substitution of the silicon atom by a carbon atom. The bonding angles also decrease from 99.25 (for **7**) to 95.26° (for **9**) in the case of P–Ni–P and from 126.92 (for **7**) to 91.21° (for **9**) in the case of Cl–Ni–Cl. The structural features suggest that the substitution of the quaternary carbon atom by a silicon atom allows for altering the donating ability of the ligand without altering the bulkiness of the donor atoms.

To test whether complexes **7** and **9** can interconvert between square-planar and tetrahedral geometry, as reported for **4**,^[24,25] we investigated the temperature dependence of the conformational preferences of complexes **7** and **9** by measuring their absorption spectra in acetonitrile at different temperatures (20–70 °C). At room temperature, both complexes show different UV/Vis spectra (Figure 2). Complex **7** displays bands at 830, 487, and 383 nm, which are characteristic for tetrahedral nickel complexes, whereas compound **9** shows a single band at 466 nm, which is indicative of a square-planar coordination environment around the Ni center. Increasing or decreasing the temperature does not alter the spectral features of both complexes, which implies that their conformations are stable and do not interconvert in solution (Figures S2 and S3). This observation was further supported by the magnetic moments determined by using the Evans method in acetonitrile. Paramagnetic **7** has a magnetic moment of 3.13 μ_B , which is con-

sistent with the theoretical value of $2.83 \mu_B$ expected for a tetrahedral Ni^{II} center, whereas **9** does not exhibit a magnetic moment, because it is diamagnetic, as expected for a low-spin square-planar Ni^{II} complex.

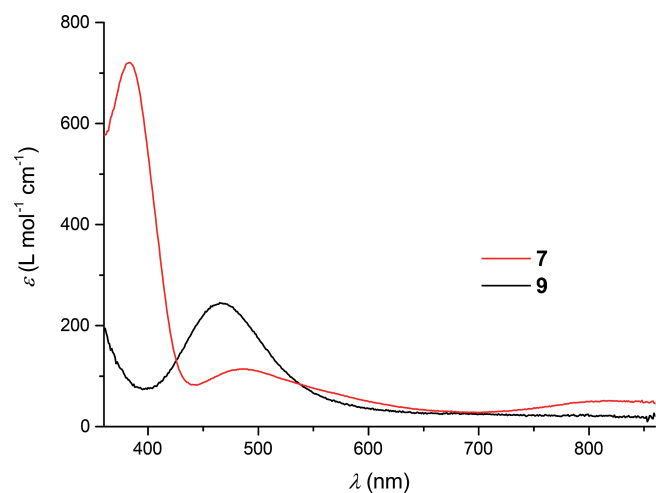


Figure 2. UV/Vis spectra of compounds **7** and **9** in acetonitrile.

To better understand the origin of the structural preferences induced by the two tripodal ligands, DFT calculations were performed. Starting from the crystal structures of **7** and **9**, we optimized the geometries of a tetrahedral and a square-planar complex for both ligands. A survey of a variety of functionals (B3LYP, PBEPBE, PBE1PBE, ω B97XD, M06-2X) revealed that only PBEPBE correctly predicts the experimentally observed preferences of a high-spin tetrahedral complex **7** ($\Delta E = 3.1$ kcal/mol) and a low-spin square-planar complex **9** ($\Delta E = 4.2$ kcal/mol). All other evaluated functionals predicted both ligands to stabilize the high-spin configuration (Table S2).

Because of this uncertainty in the prediction of energetic preferences, we decided to focus on a comparison of structural parameters of the optimized geometries. Table 1 summarizes some selected geometric parameters of the six-membered chelate ring for the four optimized structures (PBEPBE level). A close examination of the data sets shows that there are several parameters that mostly depend on either the configuration at the metal center [$d_{(Ni-P)}$, $\alpha_{(C-P-Ni)}$, $\tau_{(Ni-P-C-E)}$] or the nature of the atom E [$d_{(C-E)}$, $\alpha_{(P-Ni-P)}$]. The angle $\alpha_{(C-E-C)}$ increases by approximately $5-7^\circ$ upon going from a square-planar to a tetrahedral configuration at the metal center. However, it is important to note that this angle is overall larger for the complexes of ligand **5** than for those of ligand **6**. In fact, for the configurations found experimentally, square-planar **9** and tetrahedral **7**, the calculated angles are much closer to the ideal angle (109.4°) of a tetrahedral ER_4 unit than for the respective hypothetical structures. Therefore, $\alpha_{(C-E-C)}$, which is closely related to the distance $d_{(C-E)}$, is assumed to be the important factor determining the bonding geometry. Upon substitution of the central carbon by a silicon atom, $d_{(C-E)}$ increases from 1.55 to 1.90 Å. Consequently, the angle $\alpha_{(C-E-C)}$ would need to sharpen to maintain a square-

planar geometry. Because this is energetically less favorable, $\alpha_{(C-E-C)}$ remains close the ideal angle. Instead, an elongation of the C–E bond makes it more similar in length compared to the Ni–P bonds on the opposite side of the six-membered chelate ring. This allows the ring to convert to a more favorable chair conformation. This, in turn, decreases $\alpha_{(C-P-Ni)}$, thus improving the σ donation from the p lone pairs and forcing the nickel center into a high-spin state. Hence, it is the longer C–Si bonds that decrease the steric tension in the six-membered chelate ring and allow **7** to adopt a chair conformation and a high-spin state.

Table 1. Selected bond lengths d [Å], bond angles α [$^\circ$], and torsion angles τ [$^\circ$] of the optimized geometries^[a] of low-spin square-planar (sqpl) and high-spin tetrahedral (tetrah) forms of complexes **7** and **9** [PBEPBE/6-31G(2d,p)].

	sqpl 9	tetrah 9 ^[b]	sqpl 7 ^[b]	tetrah 7
$d_{(P-C)}$	1.87	1.86	1.86	1.83
	1.86	1.85	1.85	
$d_{(C-E)}$	1.54	1.55	1.90	1.90
			1.89	
$d_{(Ni-P)}$	2.11	2.19	2.12	2.20
			2.13	
$\alpha_{(P-Ni-P)}$	99.2	98.9	103.8	104.4
$\alpha_{(C-E-C)}$	108.7	113.2	101.1	108.6
$\alpha_{(C-P-Ni)}$	118.7	109.6	121.5	111.2
	119.7	109.9	121.6	111.1
$\tau_{(Ni-P-C-E)}$	41.4	58.5	39.4	57.8
	-37.1	-55.1	-37.8	-58.4

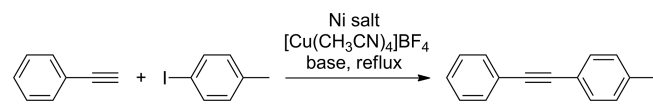
[a] Some values differ for the two binding arms, because the third unbound arm breaks the symmetry of the six-membered ring. [b] Hypothetical structures.

However, because steric tension appears to be the key factor determining the spin-state change of the nickel center, it is not surprising that the complex mixture of dispersion interactions and electronic configurations at the metal center leads to false results in the DFT-based predictions.

Beletskaya et al. reported that compound **4** is an excellent catalyst for the Cu^I-assisted coupling of 4-iodotoluene and phenyl acetylene in dioxane/water mixtures with 5 mol-% catalyst loading.^[16] In our hands, however, yields were considerably lower. We noticed that when Cu^I was replaced with $[Cu(CH_3CN)_4]BF_4$, the yields of 1-methyl-4-(phenylethynyl)benzene could be enhanced. Under these conditions, we tested the capability of the different nickel complexes in catalyzing the Sonogashira coupling of 4-iodotoluene and phenyl acetylene in water (Table 2). Whereas the reaction catalyzed by **4** gave 1-methyl-4-(phenylethynyl)benzene in 57% yield, reactions in the presence of **9** or **10** did not afford any coupling product. This result is consistent with previous reports that bidentate phosphine ligands reduce the catalytic activity of nickel-containing catalysts.^[16] A striking observation was made when compound **7** was tested as a catalyst under the same aqueous reaction conditions. In this case, 1-methyl-4-(phenylethynyl)benzene was obtained in 29% yield. Because both nickel complexes **7** and **9** possess comparable steric bulk at the phosphorus atoms and differ only in their coordination geometry, we believe that the tetrahedral coordination environment around nickel is an important requirement in nickel-cata-

lyzed Sonogashira coupling reactions involving chelating phosphine ligands.

Table 2. Catalytic Sonogashira coupling with 5 mol-% Ni complex.



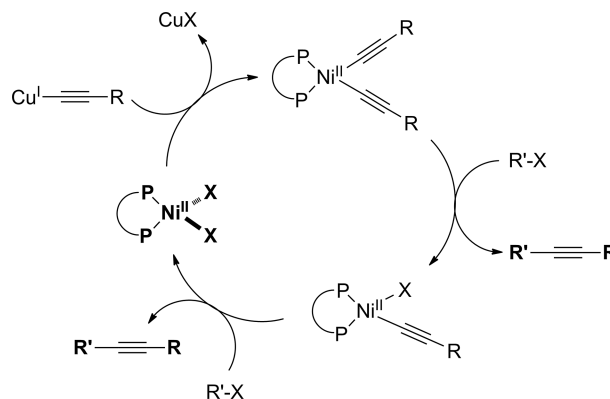
Entry	Compound	Solvent	Base	Yield [%] ^[a]
1	4	dioxane/H ₂ O	K ₂ CO ₃	57
2	9	dioxane/H ₂ O	K ₂ CO ₃	0
3	10	dioxane/H ₂ O	K ₂ CO ₃	0
4	7	dioxane/H ₂ O	K ₂ CO ₃	29
5	7	dioxane	K ₂ CO ₃	30
6 ^[b]	7	piperidine	K ₂ CO ₃	16
7	7	CH ₃ CN	K ₂ CO ₃	25
8	7	THF	K ₂ CO ₃	0
9 ^[c]	7	dioxane	K ₂ CO ₃	traces
10	7	dioxane	Cs ₂ CO ₃	29
11	8	dioxane/H ₂ O	K ₂ CO ₃	17

[a] Isolated yield, determined in triplicates. [b] Room temperature. [c] 1 mol-% Ni complex.

Next, we were interested in the solvent dependence of this coupling process in the presence of **7** (Table 2). It is notable that in polar solvents, such as dioxane/water mixtures, pure dioxane, or acetonitrile, similar yields of 1-methyl-4-(phenylethynyl)benzene were obtained. Remarkably, whereas the reactions described above require high temperature, reactions in piperidine readily proceed at room temperature (but at the cost of lower yields). In less polar solvents, no coupling products were observed. To investigate the catalytic efficiency of compound **7**, we explored the effect of catalyst loading. Unfortunately, lowering the catalyst loading to 1 mol-% lead to a trace-amount yield of the coupling product. When **7** is replaced by bromide **8**, a significantly lower yield (17%) of 1-methyl-4-(phenylethynyl)benzene was observed. This result can most likely be explained by the stronger *trans* effect of Br⁻ compared to Cl⁻, which renders the former a worse leaving group. Whereas **7** catalyzes the coupling of 4-iodotoluene and phenyl acetylene under the conditions described herein, no reaction was observed when the coupling of alkyl halides, for example, iodocyclohexane, and phenylacetylene was attempted. Likewise, when inactivated iodotoluene derivatives were used, such as 4-iodoanisole, only low yields of the desired alkynes were obtained (Scheme S1). However, this behavior can be beneficial when several functional groups are present within the molecule. For example, the coupling of 1-bromo-4-(2-bromoethyl)benzene afforded 1-(2-bromoethyl)-4-(phenylethynyl)benzene (Scheme S1) as the sole coupling product.

Although the couplings were performed under non-optimized conditions, we gathered significant mechanistic insights. We believe that a mechanism (Scheme 3) comparable to that reported by Nakamura et al. is operative.^[31] The following points support this theory:

1) A one-electron oxidation can be observed at positive potentials (ca. +0.65 V) for Ni complex **7**. This oxidation



Scheme 3. Proposed mechanism for the Ni-based Sonogashira coupling.

behavior is quite similar to that observed for compound **9** (ca. +0.60 V). Therefore, an oxidative addition and stabilization of Ni^{IV} intermediates does not seem plausible as the first reaction step.

2) In the absence of Cu⁺, no coupling product could be obtained.

3) Complex **7** and **9** react readily with Cu-phenylacetylene, which suggests that transmetalation is the initial step. However, the acetylene complexes are of different nature as revealed by the different UV/Vis spectra (Figure S7).

4) It seems that only a tetrahedral (PR)₃NiX₂ (X = Cl⁻, Br⁻) complex can initiate the catalytic cycle. A similar behavior was observed by Huttner et al. for the stereoselective heterodimerization of styrene and propene.^[26]

Conclusions

In conclusion, we could show that the substitution of a carbon atom by a silicon atom within the CH₃E-(CH₂PPh)₃ ligand system (E = C or Si) has a major influence on the structure of the resulting Ni complexes. The different coordination environments were clearly shown by single-crystal X-ray diffraction analyses. Furthermore, UV/Vis as well as NMR spectroscopic investigations suggested that both complexes are locked in their conformation. This feature allowed us to investigate the lack of catalytic activity in square-planar nickel-phosphine complexes for the Sonogashira cross-coupling reaction. As an important result, it was found that a tetrahedral (PR)₃NiCl₂ moiety is required to allow for Sonogashira cross-coupling reactions. The herein presented result might help to find and design phosphine-based Ni complexes as cheap, water-soluble, and robust catalysts for this important process.

Experimental Section

General: All reactions were performed under a dry N₂ or Ar atmosphere by using standard Schlenk techniques or by working in a Glovebox. ¹H, ¹³C{¹H}, and ³¹P{¹H} NMR spectra were recorded with a Bruker DPX-200 NMR or a Bruker DPX-250 NMR spectrometer at room temperature. Peaks were referenced to residual

^1H signals from the deuterated solvent and are reported in parts per million (ppm). $^{31}\text{P}\{^1\text{H}\}$ NMR spectra were recorded by using 85% H_3PO_4 ($\delta = 0.0$ ppm) as an external reference. Tris(chloromethyl)methylsilane^[28] and $\{2-[(\text{diphenylphosphanyl)methyl}]-2\text{-methylpropane-1,3-diyl}\}$ bis(diphenylphosphane) (Triphos, **5**)^[32] were synthesized according to literature procedures. Experimental data for compounds **8** and **10** are provided within the Supporting Information. All other compounds were obtained from commercial vendors and used without further purification. Mass spectra were obtained with either a Shimadzu QP-2010 or a Bruker Daltonics Esquire 6000 instrument. UV/Vis spectra were recorded with a Varian Cary 100 at 25 °C if not specified further. Magnetic moments were determined by using the Evans method.^[33] Prior to use, all solvents were dried according to standard methods. Thin-layer chromatography was performed by using Merck TLC aluminum sheets, silica gel 60 F_{254} . IR spectra were recorded with a Bruker Tensor IR spectrometer and are reported in cm^{-1} .

[(Methylsilylanetriyl)tris(methylene)]tris(diphenylphosphane) (Triphos^{Si}) (6): Diphenylphosphine (2.1 g, 11.3 mmol) was dissolved in THF (40 mL) and cooled to -78 °C, and *n*BuLi (7.1 mL, 11.4 mmol) was added dropwise, which resulted in a deep red reaction mixture. Subsequently, tris(chloromethyl)methylsilane (719 mg, 3.76 mmol) was added, and the mixture was stirred for 30 min at -78 °C. The solution was then warmed up overnight, whereupon the solution decolorized. Quenching of the reaction with water (1 mL) was followed by extraction with diethyl ether (3×100 mL). The organic fractions were combined and dried with Na_2SO_4 , and the solvents were evaporated to dryness. The residue was then recrystallized from methanol to afford compound **6** as a white solid (1.34 g, 56%). ^1H NMR (250 MHz, CDCl_3): $\delta = 7.33\text{--}7.18$ (m, 30 H, C_6H_5), 1.20 (s, 6 H, CH_2), 0.37 (s, 3 H, CH_3) ppm. ^{13}C NMR (50 MHz, CDCl_3): $\delta = 142.4, 133.8, 129.7$ (C_6H_5), 15.3 (CH_2), 0.0 (CH_3) ppm. ^{31}P NMR (250 MHz, CDCl_3): $\delta = -23.1$ (PPh_2) ppm. ESI-MS: calcd for $[\text{C}_{40}\text{H}_{39}\text{P}_3\text{Si} + \text{Na}]^+$ 663.2; found 663.0. $\text{C}_{40}\text{H}_{39}\text{P}_3\text{Si}$ (640.76): calcd. C 74.98, H 6.14; found C 74.69, H 6.49.

[(Triphos^{Si})NiCl₂] (7), Method A: Compound **6** (150 mg, 0.23 mmol) was dissolved in dry THF/DMF (1:1, 5 mL), and NiCl_2 (30 mg, 0.23 mmol) was subsequently added. The resulting solution was stirred for 24 h at room temperature. From the obtained dark red solution, the solvent was evaporated to dryness, and the residue was recrystallized from DMF/hexane/diethyl ether. The resulting dark red crystals were filtered off, washed with hexane and diethyl ether, and dried in vacuum to afford crystalline material (135 mg, 76%).

Method B: Compound **6** (150 mg, 0.23 mmol) was dissolved in dry THF/DMF (1:1), and $\text{Ni}(\text{PPh}_3)_2\text{Cl}_2$ (153 mg, 0.23 mmol) was subsequently added. The resulting dark red solution was stirred for 24 h. Subsequently, half of the solvent was removed under reduced pressure. Crystallization was initiated by layering the resulting solution with hexane/diethyl ether. Red crystals were separated, washed with hexane and diethyl ether, and dried to yield compound **7** (133 mg, 75%). ESI-MS: calcd for $[\text{C}_{40}\text{H}_{39}\text{Cl}_2\text{NiP}_3\text{Si} - \text{Cl}]^+$ 733.11; found 733. IR (KBr): $\tilde{\nu} = 3049, 2923, 2852, 1643, 1481, 1433, 1241, 1122, 982, 813, 697$ cm^{-1} . $\text{C}_{40}\text{H}_{39}\text{Cl}_2\text{NiP}_3\text{Si} \cdot \text{H}_2\text{O}$: calcd. C 60.94, H 5.24; found C 60.98, H 4.86.

[(Triphos)NiCl₂] (9): Nickel complex **9** was synthesized according to a modified literature procedure^[30] and as reported for compound **7**.

Method A: Compound **5** (200 mg, 0.32 mmol) and NiCl_2 (41 mg, 0.32 mmol) reacted according to *method A* (described for **7**) to yield an orange solid (93 mg, 38%).

Method B: Compound **5** (150 mg, 0.24 mmol) and $\text{Ni}(\text{PPh}_3)_2\text{Cl}_2$ (156 mg, 0.24 mmol) reacted according to *method B* (described for **7**) to yield an orange solid (158 mg, 88%). ESI-MS: calcd. for $[\text{C}_{41}\text{H}_{39}\text{Cl}_2\text{NiP}_3 - \text{Cl}]^+$ 717.13; found 717. IR (KBr): $\tilde{\nu} = 3053, 2961, 1668, 1480, 1432, 1186, 1095, 997, 838, 744, 692$ cm^{-1} . $\text{C}_{41}\text{H}_{39}\text{Cl}_2\text{NiP}_3$ (754.30): calcd. C 65.29, H 5.21; found C 65.21, H 5.48.

[(Triphos^{Si})NiBr₂] (8): Compound **6** (50 mg, 0.078 mmol) was dissolved in dry THF (2 mL), and nickel(II) bromide (22 mg, 0.078 mmol) was subsequently added. The resulting dark red solution was stirred overnight. The mixture was reduced to half of its original volume by evaporation of the solvent and subsequently filtered, and precipitation was initiated by adding Et_2O to give a brownish solid. The solid was recrystallized from DMF by Et_2O diffusion. The red crystals were separated, washed with Et_2O , and dried to afford complex **8** (37 mg, 55%). ESI-MS: calcd. for $\text{C}_{40}\text{H}_{39}\text{Br}_2\text{NiP}_3\text{Si}$ 855.98; found 777.09 $[\text{M} - \text{Br}]^+$. $\text{C}_{40}\text{H}_{39}\text{Br}_2\text{NiP}_3\text{Si}$ (859.27): calcd. C 55.91, H 4.58; found C 55.62, H 4.73.

[(Triphos)NiBr₂] (10): Compound **5** (50 mg, 0.08 mmol) was dissolved in dry THF (2 mL), and nickel(II) bromide (22 mg, 0.08 mmol) was subsequently added. The resulting dark red solution was stirred overnight. The mixture was reduced to half of its original volume by evaporation of the solvent and subsequently filtered. Precipitation was induced by adding Et_2O , which gave an orange solid. The solid was separated, washed with Et_2O , and dried to afford complex **10** (37 mg, 71%). ESI-MS: calcd. for $\text{C}_{41}\text{H}_{39}\text{Br}_2\text{NiP}_3$ 843.19; found 762.85 $[\text{M} - \text{Br}]^+$; calcd. for $\text{C}_{41}\text{H}_{39}\text{Br}_2\text{NiP}_3$: 840.00; found 761.09 $[\text{M} - \text{Br}]^+$. $\text{C}_{40}\text{H}_{39}\text{Br}_2\text{NiP}_3\text{Si}$ (859.27): calcd. C 64.52, H 5.15; found C 64.77, H 5.23.

Sonogashira Coupling. 1-Methyl-4-(phenylethynyl)benzene: In an exemplary reaction, a degassed solution of 4-iodotoluene (130 mg, 0.6 mmol), phenyl acetylene (73 mg, 0.72 mmol), K_2CO_3 (165 mg, 1.2 mmol), Ni complex (5 mol-%), and $[\text{Cu}(\text{CH}_3\text{CN})_4]\text{BF}_4$ (10 mol-%) in a mixture of 1,4-dioxane and Distilled water (3:1) was stirred for 12 h and heated at reflux. The solvent was removed under reduced pressure, and the coupling product was isolated by column chromatography (PE/ CHCl_3 , 15:1). ^1H NMR (200 MHz, CDCl_3): $\delta = 7.48\text{--}7.06$ (m, 10 H, H_{aromatic}), 2.30 (s, 3 H, CH_3) ppm. ^{13}C NMR (50 MHz, CDCl_3): $\delta = 138.4, 131.1, 131.5, 129.3, 128.2, 123.2, 120.4$ ($\text{C}_{\text{aromatic}}$), 89.0, 88.3 (C_{alkyne}), 21.5 (CH_3) ppm.

X-ray Data Collection and Structure Solution Refinement: Crystals of **7–9** were obtained by slow diffusion of diethyl ether into solutions of the compounds dissolved in DMF/hexane. Single crystals suitable for X-ray diffraction analysis were coated with Paratone-N oil, mounted on a fiber loop, and placed in a cold, gaseous N_2 stream on a Rigaku XtlabMini diffractometer performing ϕ and ω scans at 170(2) K. Diffraction intensities were measured by using graphite-monochromated Mo- K_α radiation ($\lambda = 0.71073$ Å). Data collection, indexing, initial cell refinements, frame integration, final cell refinements, and absorption corrections were performed with the program CrystalClear.^[5] Space groups were assigned by analysis of the metric symmetry and systematic absences (determined by XPREP) and were further checked for additional symmetry by using PLATON.^[34,35] Structures were solved by using direct methods and refined against all data in the reported 2θ ranges by using full-matrix least-squares methods on F^2 with the SHELXL program suite^[36] and the OLEX2 interface or the OLEX2 refinement program.^[37] Crystallographic data as well as refinement parameters are presented in Table S1 in the Supporting Information.

Electrochemistry. Instrumentation and Procedures: Cyclic voltammograms were recorded by using a non-aqueous Ag/Ag^+ reference electrode (0.1 M (*n*Bu₄N)(PF₆) and 0.01 M AgNO_3 in acetonitrile as

the supporting electrolyte]. A glassy carbon (GC) macroelectrode and a platinum wire were used as the working and auxiliary electrodes, respectively. A solution of [$n\text{Bu}_4\text{N}$][PF₆] (0.1 M, Fluka, electrochemical grade) in acetonitrile (Aldrich, anhydrous, 99.8%) was used as the supporting electrolyte. Electrochemical experiments were carried out by using a Reference 600 (Gamry Instruments, Warminster, U.S.A.) electrochemical potentiostat. Prior to each experiment, the electrochemical cell was degassed for at least 10 min by using argon, and a blanket of argon was maintained throughout the measurement. The GC working electrode was prepared by successive polishing with 1.0 and 0.3 μm alumina pastes and sonicated in Millipore water for 5 min. All cyclic voltammograms were recorded at a scan rate of 100 mV s^{-1} , and potentials reported in this paper are referenced to the ferrocenium/ferrocene couple, which was measured at the beginning of a series of experiments.

Density Functional Theory (DFT) Calculations: All DFT calculations were performed by using the Gaussian09 D.01 software package.^[38] Input structures were prepared on the basis of the crystal structures of **7** and **9**. The geometries were optimized with different functionals (B3LYP, PBEPBE, PBE1PBE, ωB97XD , M06-2X) and the 6-31G(2d,p) and 6-31+G(2d,p) basis set for all atoms under tight convergence criteria and with an ultrafine integration grid. For some calculations, implicit solvent effects were taken into account by using the polarizable continuum model^[39] (IEFPCM) for acetonitrile.

Supporting Information (see footnote on the first page of this article): MS spectra, X-ray structural analyses, UV/Vis spectra, and DFT calculations.

Acknowledgments

This work was supported by the German Fonds of the Chemical Industry (Liebig grant to C. M. and U.-P. A.) and the German Deutsche Forschungsgemeinschaft (DFG) (Emmy Noether grant to U.-P. A., AP242/2-1). Support by the DFG through the Cluster of Excellence “Ruhr Explores Solvation” (RESOLV, EXC 1069) is also gratefully acknowledged.

- [1] L. de Vega, S. van Cleuvenbergen, G. Depotter, E. M. García-Frutos, B. Gómez-Lor, A. Omenat, R. M. Tejedor, J. L. Serano, G. Henrich, K. Clays, *J. Org. Chem.* **2012**, *77*, 10891–10896.
- [2] S. Yokoshima, *Chem. Pharm. Bull.* **2013**, *61*, 251–257.
- [3] R. Hu, J. W. Y. Lam, B. Z. Tang, *Macromol. Chem. Phys.* **2013**, *214*, 175–187.
- [4] E. Negishi, L. Anastasia, *Chem. Rev.* **2003**, *103*, 1979–2018.
- [5] R. Chinchilla, C. Nájera, *Chem. Rev.* **2007**, *107*, 874–922.
- [6] R. Chinchilla, C. Nájera, *Chem. Soc. Rev.* **2011**, *40*, 5084–5121.
- [7] M. Bakherad, *Appl. Organomet. Chem.* **2013**, *27*, 125–140.
- [8] M. Eckhardt, G. C. Fu, *J. Am. Chem. Soc.* **2003**, *125*, 13642–13643.
- [9] G. Altmann, S. Würtz, F. Glorius, *Tetrahedron Lett.* **2006**, *47*, 2925–2928.
- [10] O. Vechorkin, D. Barmaz, V. Proust, X. Hu, *J. Am. Chem. Soc.* **2009**, *131*, 12078–12079.
- [11] O. Vechorkin, A. Godinat, R. Scopelliti, X. Hu, *Angew. Chem. Int. Ed.* **2011**, *50*, 11777–11781.
- [12] B. M. Rosen, K. W. Quasdorf, D. A. Wilson, N. Zhang, A.-M. Resmerita, N. K. Garg, V. Percec, *Chem. Rev.* **2011**, *111*, 1346–1416.
- [13] S. Z. Tasker, E. A. Standley, T. F. Jamison, *Nature* **2014**, *509*, 299–309.
- [14] D. Gallego, A. Brück, E. Irran, F. Meier, M. Kaupp, M. Driess, J. F. Hartwig, *J. Am. Chem. Soc.* **2013**, *135*, 15617–15626.
- [15] J. Yi, X. Lu, Y.-Y. Sun, B. Xiao, L. Liu, *Angew. Chem. Int. Ed.* **2013**, *52*, 12409–12413.
- [16] I. P. Beletskaya, G. V. Latyshev, A. V. Tsvetkov, N. V. Lukashev, *Tetrahedron Lett.* **2003**, *44*, 5011–5013.
- [17] J. W. Dankwardt, *Angew. Chem. Int. Ed.* **2004**, *43*, 2428–2432; *Angew. Chem.* **2004**, *116*, 2482.
- [18] M. Jeganmohan, C.-H. Cheng, *Chem. Eur. J.* **2008**, *14*, 10876–10886.
- [19] M. Tobisu, T. Shimasaki, N. Chatani, *Angew. Chem. Int. Ed.* **2008**, *47*, 4866–4869; *Angew. Chem.* **2008**, *120*, 4944.
- [20] J. Canivet, J. Yamaguchi, I. Ban, K. Itami, *Org. Lett.* **2009**, *11*, 1733–1736.
- [21] K. Muto, J. Yamaguchi, K. Itami, *J. Am. Chem. Soc.* **2012**, *134*, 169–172.
- [22] M. Bakherad, A. Keivanloo, S. Mihanparast, *Synth. Commun.* **2009**, *40*, 179–185.
- [23] L. Cassar, *J. Organomet. Chem.* **1975**, *93*, 253–257.
- [24] B. Corain, B. Longato, R. Angeletti, G. Valle, *Inorg. Chim. Acta* **1985**, *104*, 15–18.
- [25] L. Brammer, E. D. Stevens, *Acta Crystallogr., Sect. C* **1989**, *45*, 400–403.
- [26] R. Faissner, G. Huttner, *Eur. J. Inorg. Chem.* **2003**, 2239–2244.
- [27] A. Muth, O. Walter, G. Huttner, A. Asam, L. Zsolnai, C. Emmerich, *J. Organomet. Chem.* **1994**, *468*, 149–163.
- [28] U.-P. Apfel, D. Troegel, Y. Halpin, S. Tschierlei, U. Uhlemann, H. Görls, M. Schmitt, J. Popp, P. Dunne, M. Venkatesan, M. Coey, M. Rudolph, J. G. Vos, R. Tacke, W. Weigand, *Inorg. Chem.* **2010**, *49*, 10117–10132.
- [29] L. M. Venanzi, *J. Chem. Soc.* **1958**, 719–724.
- [30] M. Kandiah, G. S. McGrady, A. Decken, P. Sirsch, *Inorg. Chem.* **2005**, *44*, 8650–8652.
- [31] T. Hatakeyama, Y. Okada, Y. Yoshimoto, M. Nakamura, *Angew. Chem. Int. Ed.* **2011**, *50*, 10973–10976.
- [32] S. Herold, A. Mezzetti, L. M. Venanzi, A. Albinati, F. Lianza, T. Gerfin, V. Gramlich, *Inorg. Chim. Acta* **1995**, *235*, 215–231.
- [33] D. F. Evans, *J. Chem. Soc.* **1959**, 2003–2005.
- [34] A. L. Spek, *J. Appl. Crystallogr.* **2003**, *36*, 7–13.
- [35] A. L. Spek, *Acta Crystallogr., Sect. D* **2009**, *65*, 148–155.
- [36] G. M. Sheldrick, *Acta Crystallogr., Sect. A* **2008**, *64*, 112–122.
- [37] O. V. Dolomanov, L. J. Bourhis, R. J. Gildea, J. A. K. Howard, H. Puschmann, *J. Appl. Crystallogr.* **2009**, *42*, 339–341.
- [38] M. J. Frisch, G. W. Trucks, H. B. Schlegel, G. E. Scuseria, M. A. Robb, J. R. Cheeseman, G. Scalmani, V. Barone, B. Mennucci, G. A. Petersson, H. Nakatsuji, M. Caricato, X. Li, H. P. Hratchian, A. F. Izmaylov, J. Bloino, G. Zheng, J. L. Sonnenberg, M. Hada, M. Ehara, K. Toyota, R. Fukuda, J. Hasegawa, M. Ishida, T. Nakajima, Y. Honda, O. Kitao, H. Nakai, T. Vreven, J. J. A. Montgomery, J. E. Peralta, F. Ogliaro, M. Bearpark, J. J. Heyd, E. Brothers, K. N. Kudin, V. N. Staroverov, T. Keith, R. Kobayashi, J. Normand, K. Raghavachari, A. Rendell, J. C. Burant, S. S. Iyengar, J. Tomasi, M. Cossi, N. Rega, J. M. Millam, M. Klene, J. E. Knox, J. B. Cross, V. Bakken, C. Adamo, J. Jaramillo, R. Gomperts, R. E. Stratmann, O. Yazyev, A. J. Austin, R. Cammi, C. Pomelli, J. W. Ochterski, R. L. Martin, K. Morokuma, V. G. Zakrzewski, G. A. Voth, P. Salvador, J. J. Dannenberg, S. Dapprich, A. D. Daniels, O. Farkas, J. B. Foresman, J. V. Ortiz, J. Cioslowski, D. J. Fox, *Gaussian, Inc.*, Wallingford CT **2013**.
- [39] J. Tomasi, B. Mennucci, R. Cammi, *Chem. Rev.* **2005**, *105*, 2999–3094.

Received: February 11, 2015
Published Online: March 18, 2015